Optical Engineering 49(3), 033602 (March 2010)

Color quality scale

Wendy Davis
Yoshi Ohno
National Institute of Standards and Technology
100 Bureau Drive, MS 8442
Gaithersburg, Maryland 20899-8442
E-mail: wendy.davis@nist.gov

Abstract. The color rendering index (CRI) has been shown to have deficiencies when applied to white light-emitting-diode–based sources. Furthermore, evidence suggests that the restricted scope of the CRI unnecessarily penalizes some light sources with desirable color qualities. To solve the problems of the CRI and include other dimensions of color quality, the color quality scale (CQS) has been developed. Although the CQS uses many of elements of the CRI, there are a number of fundamental differences. Like the CRI, the CQS is a test-samples method that compares the appearance of a set of reflective samples when illuminated by the test lamp to their appearance under a reference illuminant. The CQS uses a larger set of reflective samples, all of high chroma, and combines the color differences of the samples with a root mean square. Additionally, the CQS does not penalize light sources for causing increases in the chroma of object colors but does penalize sources with smaller rendered color gamut areas. The scale of the CQS is converted to span 0–100, and the uniform object color space and chromatic adaptation transform used in the calculations are updated. Supplementary scales have also been developed for expert users. [DOI: 10.1117/1.3360335]

Subject terms: colorimetry; color rendering; light-emitting diodes.

Paper 090748PR received Sep. 28, 2009; revised manuscript received Jan. 8, 2010; accepted for publication Jan. 13, 2010; published online Mar. 30, 2010.

1 Introduction

Color rendering is defined by the International Commission on Illumination (CIE) as the "effect of an illuminant on the color appearance of objects by conscious or subconscious comparison with their color appearance under a reference illuminant."[1] The CIE color rendering index[2] (CRI) is widely used and the only internationally accepted metric for assessing the color-rendering performance of light sources. The CRI was developed in the middle of the twentieth century to evaluate the color-rendering performance of then-new fluorescent lamps. Recent momentum to commercialize lamps using light-emitting diodes (LEDs) for general illumination is exposing some shortcomings of the CRI, some of which are particularly prominent when applied to LEDs.[3,4] These observations have led to the development of a color quality scale (CQS), which aspires to solve the problems of the CRI, be applicable to all light source technologies, and evaluate aspects of color quality beyond color rendering.

In the calculation of the CRI, the color appearance of 14 reflective samples is calculated when illuminated by a reference illuminant and the test light source. The simulated color of the 14 samples, when illuminated by a CIE Daylight illuminant of 6500 K (D65), is shown in Fig. 1.

For the CRI calculations, the reference illuminant is a Planckian radiator (if <5000 K) or a CIE Daylight illuminant (if $\geqslant 5000$ K), matched to the correlated color temperature (CCT) of the test source. After accounting for chromatic adaptation with a Von Kries correction, the difference in color appearance (ΔE_i) for each sample between illumination by the test source and the reference illuminant is computed in CIE 1964 $W^*U^*V^*$ uniform color space. The Special CRI (R_i) is calculated for each reflective sample (i) by

$$R_i = 100 - 4.6\Delta E_i. \tag{1}$$

The General CRI (R_a) is simply the average of R_i for the first eight samples, all of which have low to moderate chromatic saturation [shown in Fig. 1(a)]

$$R_a = \frac{1}{8}\sum_{i=1}^{8} R_i. \tag{2}$$

A perfect score of 100 represents no color differences in any of the eight samples under the test source and reference illuminant.

The CRI has a number of shortcomings and problems. The uniform color space used to calculate color differences is outdated and no longer recommended for use. The red region of this color space is particularly nonuniform. Instead, the CIE currently recommends CIE 1976 $L^*a^*b^*$ (CIELAB) and CIE 1976 $L^*u^*v^*$ (CIELUV)[5] for calculating object color differences. The chromatic adaptation transform used by the CRI is also considered obsolete and inadequate. The Von Kries chromatic adaptation correction has been shown to perform poorer than other available models, such as the Colour Measurement Committee's Chromatic Adaptation Transform of 2000 (CMCCAT2000) and the CIE's Chromatic Adaptation Transform (CIE CAT02).[6]

The CRI method specifies that the CCT of the reference illuminant be matched to that of the test source, which as-

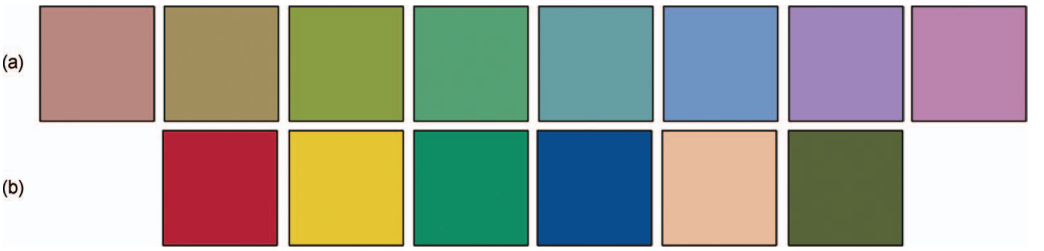

Fig. 1 Simulated color appearance of 14 CRI reflective samples when illuminated by D65. The eight samples used in the calculation of R_a are in the top row.

sumes complete chromatic adaptation to any light source CCT. This assumption fails at extreme CCTs, however. For example, a 2000-K (very reddish) blackbody source would achieve a CRI R_a=100. However, the colors of objects illuminated by such a source would appear distorted.

None of the eight reflective samples used in the computation of R_a are highly saturated. This can be problematic, especially for red-green-blue (RGB) white LEDs with strong peaks and pronounced valleys in their spectra. Color rendering of saturated colors can be very poor even when rendering of desaturated colors is good, which would result in a high R_a value. RGB LEDs have the potential to be highly energy efficient, but poor color rendering would inhibit their market acceptance. Developers of these light sources need an effective metric to evaluate the color rendering of RGB LED sources and LED luminaires.

The eight Special Color Rendering Indices are combined by a simple averaging to obtain the General Color Rendering Index. This makes it possible for a lamp to score quite well, even when it renders one or two colors very poorly. Again, RGB LEDs are at an increased risk of being affected by this problem, because their unique spectra are more vulnerable to poor rendering in only certain areas of color space. These problems also apply to phosphor-type white LEDs if narrowband phosphors are used, as most fluorescent lamps currently use, as well as any other current or future light source employing narrowband radiation.

Finally, the very definition of color rendering is limiting. Color rendering is a measure of only the fidelity of object colors under the source of interest, and any deviation of object color appearance from under a blackbody or daylight illuminant is considered bad. Because of this constraint, all shifts in perceived object hue, saturation, and lightness result in equal decrements of the R_a score. In practical application, however, increases in the chromatic saturation of reflective objects, observed when certain sources illuminate certain surfaces, are considered desirable. Increases in saturation yield better visual clarity and enhance perceived brightness.[7,8]

A couple of computational examples from white LED simulations[3] illustrate the deficiencies and limitations of the CRI. First, consider an RGB LED with peaks at 466, 538, and 603 nm. Its spectrum is shown in Fig. 2(a). This source would have a CCT of 3300 K and would receive a CRI R_a of 80. This R_a is generally considered rather high, and most users would trust that the source is a good color renderer. However, this RGB LED would render saturated red and purple object colors very poorly, as shown in the CIELAB plot of 15 saturated object colors in Fig. 2(b). This is a two-dimensional (a^*,b^*) CIELAB plot: the origin represents a neutral gray, the distance from the origin represents object chroma (similar to saturation), and the angle represents object hue. The gray line connecting the circles shows the object colors under the reference illuminant, and the black line connecting the squares shows them when illuminated by the test source. The positive a^*-axis roughly corresponds to red hues, and it is clear that the chroma of reddish objects is markedly decreased under the test source. In this case, the fact that the CRI uses relatively desaturated

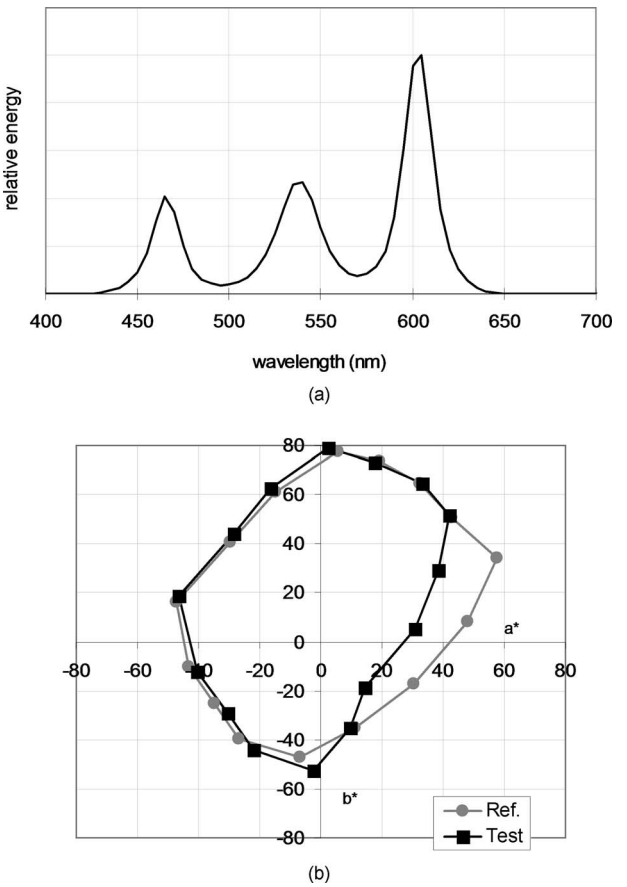

Fig. 2 (a) Spectrum of RGB LED with peaks at 466, 538, and 603 nm. (b) CIELAB plot of color rendering performance with 15 saturated reflective samples. The gray circles plot sample color under the reference illuminant, and the black squares show sample color under the test source.

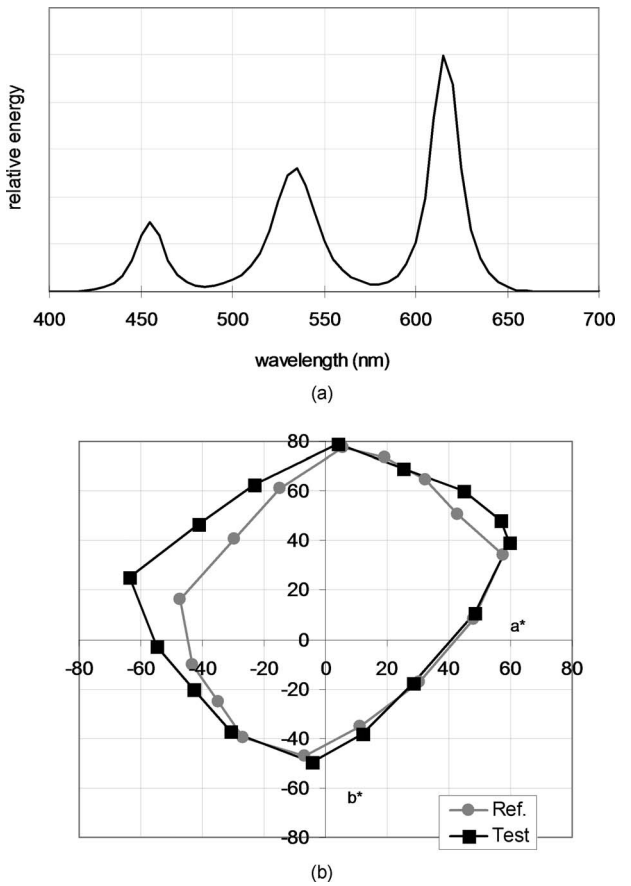

Fig. 3 (a) Spectrum of RGB LED with peaks at 455, 534, and 616 nm. (b) CIELAB plot of color rendering performance with 15 saturated reflective samples. The gray circles plot sample color under the reference illuminant, and the black squares show sample color under the test source.

reflective samples and combines the Special Color Rendering Indices by averaging leads to an inappropriately high R_a score.

The spectrum of a slightly different RGB LED is shown in Fig. 3(a). In this case, the peaks are at 455, 534, and 616 nm and the CCT would also be 3300 K. However, the CRI R_a for this RGB LED would be only 67, a fairly low score that many users may not consider suitable for certain color-important applications. However, the CIELAB plot in Fig. 3(b) reveals that the primary deviations in object color caused by the test source are increases in object chroma for green, turquoise, orange, and red colors. In real life, this light source would not appear very bad to most users and, in some cases, would be preferred. This RGB LED source illustrates the potential benefits of increasing the scope of a new metric from the strict definition of color rendering to include other dimensions of color quality.

2 Guiding Principles

A number of basic tenets directed the development of the CQS. They are based on both practical and theoretical considerations. To fully understand the reasoning behind the different elements of the CQS, a brief description of these guiding principles is warranted.

The CQS was modeled after the CRI to the extent that was reasonably possible without sacrificing metric performance. The CRI has been used in the lighting industry for decades, and in spite of its problems, many users have been content with it. The decision to develop a new metric that has "the look and feel" of the familiar CRI not only provided a useful starting point for the development of the CQS, but hopefully will aid in industry adoption.

Though a major motivation for the replacement of the CRI is its relatively poor performance with some LED light sources, the CQS was developed to evaluate color quality for all types of light sources. The comparison of lighting products of differing technologies will only be possible if all light sources are evaluated with the same metric. Furthermore, the goal was established to maintain consistency of average scores with the CRI for fluorescent lamps. This was a practical consideration, because the CRI is widely used and accepted among fluorescent lamp manufacturers. It was anticipated that a new metric with widely disparate outputs could suffer from a lack of market acceptance and use.

Unlike the CRI, which only considers the fidelity of object colors under the test source, the new metric would seek to integrate other dimensions of color quality. Evidence has accumulated over the years that object colors that actually deviate from perfect fidelity often "look better" to people. That is, certain shifts in hue or chroma of object colors are preferred by observers. This was the basis of the Flattery Index, a metric proposed by Judd in 1967.[9] He compiled the results of previous psychology studies to determine the preferred color shifts for common objects. For example, the preferred color of Caucasian skin is redder and more saturated than true fidelity.[10] The colors of green leaves and grass are preferred to appear less yellow and slightly more saturated than they really are.[11] These findings were also the basis for the proposed Color Preference Index (CPI).[12] More recent research has indicated that object colors are often remembered as being slightly more saturated than they really are,[13] suggesting that humans' idealized or preferred object colors have a higher chromatic saturation than the real objects. A later proposal suggested combining elements of the CPI and CRI into a single CPI-CRI.[14]

The illuminance of the lit environment has a profound effect on object colors, but cannot reasonably be integrated into a color-quality metric, which needs to be applicable to individual light sources, independent of their ultimate applications. Even if it is known that a given light bulb emits 3000 lumens, it is not known how far away from the user the bulb will be installed or whether it will be installed with other light sources. As a practical matter, illuminance cannot be integrated into a color-quality metric. However, it is reasonable to assume that the environments in which the artificial light sources are used will be substantially dimmer than outdoor daylight conditions. Indoor artificial lighting environments are commonly 50–500 lux, while daylight outdoors can be up to 100,000 lux. If daylight is considered to be humans' "ultimate reference illuminant," as an overwhelming portion of human evolution relied on daylight as the primary light source, then it could also be concluded that objects illuminated by daylight are the most natural looking. The perceived hues of colors are dependent on illuminance (Bezold–Brucke effect),[15] and colors appear

more saturated under higher illuminances (Hunt effect).[16] Therefore, if an artificial light source increases object saturation (relative to the reference illuminant), the object may actually appear more like it would when illuminated by real daylight. This may make the object actually appear more natural to observers.

The ability to distinguish between similar colors, chromatic discrimination is another dimension of color quality that can deviate from absolute fidelity. The number of object colors that a light source permits discrimination between can be inferred by the gamut area (of rendered object colors) of the light source. For instance, if one selects a set of reflective samples and plots them in CIELAB with different light sources as the illuminants, the spacing between samples will be larger for some light sources, resulting in larger gamut areas, than others. When the distance between samples is larger in a uniform color space, the samples appear more different from each other (than when distances are smaller) and an observer would be able to distinguish a greater number of colors intermediate to the two samples. In addition to increased chromatic discrimination, larger object gamut areas have been associated with increased perceived brightness, enhanced visual clarity, and increased object color saturation.[17,18] Gamut area is clearly a useful measure for certain color-quality properties of light sources and has been proposed as the central component to a number of proposed color-rendering metrics.[7,19–21]

Finally, it was decided *a priori* that the new metric would yield a one-number output between zero and 100. The CRI can generate outputs with large negative numbers for very poor test sources. For instance, for a low-pressure sodium lamp, $R_a=-47$. Color rendering is virtually nonexistent with this lamp. A score of zero would effectively communicate the same message. Negative values simply do not convey any useful information and have the potential to confuse users.

The decision to restrict the output of the new metric to one number is certainly controversial. The argument has been made that it is impossible to communicate the different dimensions of quality with only one number.[22,23] Indeed, in some cases different dimensions of color quality, such as fidelity and preference, can be contradictory. A metric to assess a property like color quality inherently condenses information. After all, if the goal was to provide all possible information about how a given light source would render object colors, then one could use the spectral power distribution of the source and colorimetric formulae to determine the detailed color-rendering information (e.g., direction and magnitude of hue, chroma, and lightness shifts) of countless object colors. Even with all that information, most users would still need guidance in how to use the information to judge the suitability of a light source for a specific application. The purpose of a metric is to condense such an immense amount of information into something manageable and useful. In order to be useful for the greatest number of users, most of whom have very limited knowledge of colorimetry, a one-number output is desirable. Though most users will not know exactly how the number was determined or precisely what it means, this is readily accepted by a majority of people. Throughout the course of our lives, we use many measurement scales, whose precise meanings and measurement methodologies are unknown to us, without concern. Examples of such measurement scales include shoe sizes, octane ratings of gasoline, and radio station frequencies. Though most people do not know precisely how those numbers are determined, they find the scales useful and have a general understanding of how different outputs relate to each other (a larger shoe size means a bigger foot). However, it was acknowledged that additional outputs, for expert users needing specialized information, would be useful and should be created to supplement the one-number general output.

3 CQS

Led by these guiding principles, a method for the evaluation of light source color quality was developed through computational analyses and colorimetric simulations. The resulting metric was named the CQS, a clear nod to the CRI but sufficiently different to avoid confusion among users. A thorough account of the calculations involved in the CQS is provided here. Readers who are knowledgeable in basic colorimetry may find the level of detail to be excessive, but it was deemed important to provide complete enough information that even a colorimetry novice could carry out the calculations. A spreadsheet, with all of the calculations implemented as well as additional features, such as the display of simulated sample colors, is also available from the authors.

3.1 *Reference Illuminant*

The CQS, like the CRI, is a test-sample method. That is, color differences (in a uniform object color space) are calculated for a predetermined set of reflective samples when illuminated by a test source and a reference illuminant. In essence, through a simulation, the appearance of the object colors is determined and compared when illuminated by the test source and the reference illuminant. The reference illuminants are the same as those used by the CRI. For test sources of <5000 K, the reference illuminant is a Planckian radiator at the same CCT as the test source. These calculation procedures are given in CIE's primary colorimetry publication[5] but are repeated below. The spectrum of the Planckian reference illuminant, $S_{\mathrm{ref}}(\lambda)$, is calculated by

$$S_{\mathrm{ref}}(\lambda,T)=\frac{L_{e,\lambda}(\lambda,T)}{L_{e,\lambda}(560\ \mathrm{nm},T)}, \tag{3}$$

where T is the CCT of the test source and $L_{e,\lambda}$ is the relative spectral radiance calculated by

$$L_{e,\lambda}(\lambda,T)=\lambda^{-5}\left[\exp\left(\frac{1.4388\times10^{-2}}{\lambda T}\right)-1\right]^{-1}. \tag{4}$$

For test sources at $\geqslant5000$ K, the reference is a phase of CIE Daylight illuminant having the same CCT as the test source. The method for calculating the spectral power distribution of the daylight illuminant begins with determining the chromaticity coordinates (x_D,y_D) of the illuminant. For illuminants up to and including 7000 K, x_D is

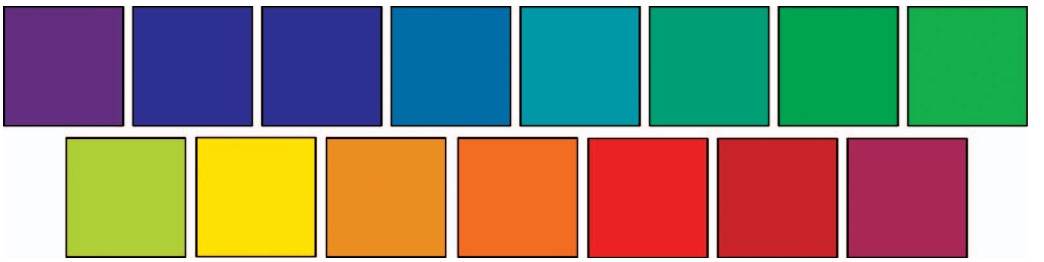

Fig. 4 Simulated color appearance of 15 CQS reflective samples when illuminated by D65.

$$x_D = \frac{-4.6070 \times 10^9}{(T_{cp})^3} + \frac{2.9678 \times 10^6}{(T_{cp})^2} + \frac{0.09911 \times 10^3}{T_{cp}} + 0.244063. \quad (5)$$

For illuminants with CCT of >7000 K, x_D is

$$x_D = \frac{-2.0064 \times 10^9}{(T_{cp})^3} + \frac{1.9018 \times 10^6}{(T_{cp})^2} + \frac{0.24748 \times 10^3}{T_{cp}} + 0.237040. \quad (6)$$

The y coordinate (y_D) is calculated by

$$y_D = -3.000x_D^2 + 2.870x_D - 0.275. \quad (7)$$

The relative spectral power distribution of the daylight reference illuminant, $S_{ref}(\lambda)$, is calculated with

$$S_{ref}(\lambda) = S_0(\lambda) + M_1 S_1(\lambda) + M_2 S_2(\lambda), \quad (8)$$

where $S_0(\lambda)$, $S_1(\lambda)$, and $S_2(\lambda)$ are functions of wavelength and are given in Table T.2 of Ref. 5. M_1 and M_2 are multiplication factors determined as follows:

$$M_1 = \frac{-1.3515 - 1.7703x_D + 5.9114y_D}{0.0241 + 0.2562x_D - 0.7341y_D}, \quad (9)$$

$$M_2 = \frac{0.0300 - 31.4424x_D + 30.0717y_D}{0.0241 + 0.2562x_D - 0.7341y_D}. \quad (10)$$

Because the tables of $S_0(\lambda)$, $S_1(\lambda)$, and $S_2(\lambda)$ are available only at 5-nm intervals, the calculation of the CQS (as well as the CRI) uses wavelength intervals of 5 nm, which is sufficient. Smaller intervals normally would not produce meaningfully different results, but if smaller interval calculations are desired in order to match the wavelength interval of spectral distribution measurement of the test source, then the $S_0(\lambda)$, $S_1(\lambda)$, and $S_2(\lambda)$ values should be interpolated using Lagrange, cubic spline, or other recommended interpolation method.[24] Calculation at intervals of >5 nm should not be used.

3.2 *Tristimulus Values*

There are 15 reflective samples used in the CQS calculations, all of which are currently commercially available Munsell samples, of the following hue value/chroma designations: 7.5 P 4/10, 10 PB 4/10, 5 PB 4/12, 7.5 B 5/10, 10 BG 6/8, 2.5 BG 6/10, 2.5 G 6/12, 7.5 GY 7/10, 2.5 GY 8/10, 5 Y 8.5/12, 10 YR 7/12, 5 YR 7/12, 10 R 6/12, 5 R 4/14, and 7.5 RP 4/12. The reflectance factors for these samples are given in Appendix A. Although it was shown earlier that light sources can perform poorly with saturated reflective samples even when they perform well with desaturated samples, extensive computational testing has revealed that the inverse is never true. That is, there is no light source spectrum that would render saturated colors well, but perform poorly with desaturated colors. This is related to some of the intrinsic properties of reflective objects. Desaturated colors have a higher broad baseline reflectance than saturated colors. In essence, that baseline is white/gray. Of course, white is relatively "easy" for a white-light source to render, because the light itself is white. Highly saturated objects lack the relatively high broad baseline, and most of their reflected light is from a much smaller segment of the visible spectrum. Therefore, the CQS sample set is limited to only saturated colors. The simulated color appearance of these samples, when illuminated by D65, is shown in Fig. 4.

The next step in calculating the CQS is to determine the tristimulus values (X, Y, and Z) of each reflective sample (i) when illuminated by the reference illuminant. In the following calculations, $R_i(\lambda)$ is the spectral reflectance factor of reflective sample i,

$$X_{i,ref} = k_{ref} \int_\lambda S_{ref}(\lambda) R_i(\lambda) \bar{x}(\lambda) d\lambda, \quad (11)$$

$$Y_{i,ref} = k_{ref} \int_\lambda S_{ref}(\lambda) R_i(\lambda) \bar{y}(\lambda) d\lambda, \quad (12)$$

$$Z_{i,ref} = k_{ref} \int_\lambda S_{ref}(\lambda) R_i(\lambda) \bar{z}(\lambda) d\lambda, \quad (13)$$

where

$$k_{ref} = 100 \Big/ \int_\lambda S_{ref}(\lambda) \bar{y}(\lambda) d\lambda. \quad (14)$$

A similar set of calculations is performed for the samples when illuminated by the test source.

$$X_{i,\text{test}} = k_{\text{test}} \int_{\lambda} S_{\text{test}}(\lambda) R_i(\lambda) \bar{x}(\lambda) d\lambda, \tag{15}$$

$$Y_{i,\text{test}} = k_{\text{test}} \int_{\lambda} S_{\text{test}}(\lambda) R_i(\lambda) \bar{y}(\lambda) d\lambda, \tag{16}$$

$$Z_{i,\text{test}} = k_{\text{test}} \int_{\lambda} S_{\text{test}}(\lambda) R_i(\lambda) \bar{z}(\lambda) d\lambda, \tag{17}$$

where

$$k_{\text{test}} = 100 \Big/ \int_{\lambda} S_{\text{test}}(\lambda) \bar{y}(\lambda) d\lambda. \tag{18}$$

These integral calculations are done numerically at 5-nm intervals.

3.3 *Chromatic Adaptation Transform*

Even though the CCT of the reference illuminant is matched to that of the test source, the chromaticity coodinates are likely different, because the test source chromaticity rarely falls exactly on the Planckain locus or Daylight locus. Thus, a chromatic adaptation transform is necessary to compensate for these types of differences in light color, as was also applied in CRI. A current chromatic adaptation transform procedure was adopted in CQS.

After calculation of the tristimulus values of the illuminated samples, these values are corrected for chromatic adaptation. The CMCCAT2000[25] is applied. The tristimulus values of a perfect diffuser illuminated by the reference illuminant ($X_{\text{w,ref}}$, $Y_{\text{w,ref}}$, $Z_{\text{w,ref}}$) and by the test source ($X_{\text{w,test}}$, $Y_{\text{w,test}}$, $Z_{\text{w,test}}$) are first calculated as the white references. For a perfect diffuser, $R(\lambda) \equiv 1$.

$$X_{\text{w,ref}} = k_{\text{ref}} \int_{\lambda} S_{\text{ref}}(\lambda) R(\lambda) \bar{x}(\lambda) d\lambda, \tag{19}$$

$$Y_{\text{w,ref}} = k_{\text{ref}} \int_{\lambda} S_{\text{ref}}(\lambda) R(\lambda) \bar{y}(\lambda) d\lambda, \tag{20}$$

$$Z_{\text{w,ref}} = k_{\text{ref}} \int_{\lambda} S_{\text{ref}}(\lambda) R(\lambda) \bar{z}(\lambda) d\lambda, \tag{21}$$

and

$$X_{\text{w,test}} = k_{\text{test}} \int_{\lambda} S_{\text{test}}(\lambda) R(\lambda) \bar{x}(\lambda) d\lambda, \tag{22}$$

$$Y_{\text{w,test}} = k_{\text{test}} \int_{\lambda} S_{\text{test}}(\lambda) R(\lambda) \bar{y}(\lambda) d\lambda, \tag{23}$$

$$Z_{\text{w,test}} = k_{\text{test}} \int_{\lambda} S_{\text{test}}(\lambda) R(\lambda) \bar{z}(\lambda) d\lambda. \tag{24}$$

Then, the tristimulus values are transformed into R, G, and B values

$$\begin{pmatrix} R_{i,\text{test}} \\ G_{i,\text{test}} \\ B_{i,\text{test}} \end{pmatrix} = M \begin{pmatrix} X_{i,\text{test}} \\ Y_{i,\text{test}} \\ Z_{i,\text{test}} \end{pmatrix}, \tag{25}$$

$$\begin{pmatrix} R_{\text{w,ref}} \\ G_{\text{w,ref}} \\ B_{\text{w,ref}} \end{pmatrix} = M \begin{pmatrix} X_{\text{w,ref}} \\ Y_{\text{w,ref}} \\ Z_{\text{w,ref}} \end{pmatrix}, \tag{26}$$

$$\begin{pmatrix} R_{\text{w,test}} \\ G_{\text{w,test}} \\ B_{\text{w,test}} \end{pmatrix} = M \begin{pmatrix} X_{\text{w,test}} \\ Y_{\text{w,test}} \\ Z_{\text{w,test}} \end{pmatrix}, \tag{27}$$

where

$$M = \begin{pmatrix} 0.7982 & 0.3389 & -0.1371 \\ -0.5918 & 1.5512 & 0.0406 \\ 0.0008 & 0.0239 & 0.9753 \end{pmatrix}. \tag{28}$$

Next, the "corresponding" R, G, and B ($R_{i,\text{test,c}}$, $G_{i,\text{test,c}}$, $B_{i,\text{test,c}}$) values are determined for each sample i,

$$R_{i,\text{test,c}} = R_{i,\text{test}} \alpha (R_{\text{w,ref}} / R_{\text{w,test}}), \tag{29}$$

$$G_{i,\text{test,c}} = G_{i,\text{test}} \alpha (G_{\text{w,ref}} / G_{\text{w,test}}), \tag{30}$$

$$B_{i,\text{test,c}} = B_{i,\text{test}} \alpha (B_{\text{w,ref}} / B_{\text{w,test}}), \tag{31}$$

where

$$\alpha = Y_{\text{w,test}} / Y_{\text{w,ref}}. \tag{32}$$

Readers familiar with CMCCAT2000 may note the absence of the variables for the lumninances of adapting fields (L_{A1} and L_{A2}) and degree of adaptation (D). Because the luminances are not knowable in this situation, they were assumed to be high and identical (e.g., 500 cd/m^2), which makes the degree of adaptation equal to 1. As these values cancelled out, they do not appear in Eqs. (29)–(32).

The corresponding tristimulus values ($X_{i,\text{test,c}}$, $Y_{i,\text{test,c}}$, $Z_{i,\text{test,c}}$) after chromatic adaptation correction are then calculated,

$$\begin{pmatrix} X_{i,\text{test,c}} \\ Y_{i,\text{test,c}} \\ Z_{i,\text{test,c}} \end{pmatrix} = M^{-1} \begin{pmatrix} R_{i,\text{test,c}} \\ G_{i,\text{test,c}} \\ B_{i,\text{test,c}} \end{pmatrix}, \tag{33}$$

where

$$M^{-1} = \begin{pmatrix} 1.076450 & -0.237662 & 0.161212 \\ 0.410964 & 0.554342 & 0.034694 \\ -0.010954 & -0.013389 & 1.024343 \end{pmatrix}. \tag{34}$$

3.4 *CIE 1976 L*a*b* Coordinates*

The uniform object color space used in the CQS calculations is CIE 1976 $L^*a^*b^*$; thus, these coordinates are calculated for each of the reflective samples (i) when illuminated by the reference illuminant ($L^*_{i,\mathrm{ref}}$, $a^*_{i,\mathrm{ref}}$, $b^*_{i,\mathrm{ref}}$). The calculation procedures are given in CIE's primary colorimetry publication,[5] but are repeated as follows:

$$L^*_{i,\mathrm{ref}} = 116\left(\frac{Y_{i,\mathrm{ref}}}{Y_{\mathrm{w,ref}}}\right)^{1/3} - 16, \tag{35}$$

$$a^*_{i,\mathrm{ref}} = 500\left[\left(\frac{X_{i,\mathrm{ref}}}{X_{\mathrm{w,ref}}}\right)^{1/3} - \left(\frac{Y_{i,\mathrm{ref}}}{Y_{\mathrm{w,ref}}}\right)^{1/3}\right], \tag{36}$$

$$b^*_{i,\mathrm{ref}} = 200\left[\left(\frac{Y_{i,\mathrm{ref}}}{Y_{\mathrm{w,ref}}}\right)^{1/3} - \left(\frac{Z_{i,\mathrm{ref}}}{Z_{\mathrm{w,ref}}}\right)^{1/3}\right]. \tag{37}$$

Note that, in the definition of CIELAB,[5] the formulae are different depending on the values of (X/X_n), (Y/Y_n), and (Z/Z_n). These conditional formulae are needed only to correct the results for very low reflectance samples. It has been computationally verified that such conditional formulae are not needed for the 15 color samples used in CQS, thus the simple formulae above are sufficient for accurate calculation for these samples.

This procedure is repeated to calculate the coordinates for each sample (i) illuminated by the test source ($L^*_{i,\mathrm{test}}$, $a^*_{i,\mathrm{test}}$, $b^*_{i,\mathrm{test}}$).

$$L^*_{i,\mathrm{test}} = 116\left(\frac{Y_{i,\mathrm{test,c}}}{Y_{\mathrm{w,test}}}\right)^{1/3} - 16, \tag{38}$$

$$a^*_{i,\mathrm{test}} = 500\left[\left(\frac{X_{i,\mathrm{test,c}}}{X_{\mathrm{w,test}}}\right)^{1/3} - \left(\frac{Y_{i,\mathrm{test,c}}}{Y_{\mathrm{w,test}}}\right)^{1/3}\right], \tag{39}$$

$$b^*_{i,\mathrm{test}} = 200\left[\left(\frac{Y_{i,\mathrm{test,c}}}{Y_{\mathrm{w,test}}}\right)^{1/3} - \left(\frac{Z_{i,\mathrm{test,c}}}{Z_{\mathrm{w,test}}}\right)^{1/3}\right]. \tag{40}$$

From these coordinates, the chroma of each sample under the reference illuminant ($C^*_{\mathrm{ab,ref}}$) and test source ($C^*_{\mathrm{ab,test}}$) is calculated as follows:

$$C^*_{i,\mathrm{ref}} = [(a^*_{i,\mathrm{ref}})^2 + (b^*_{i,\mathrm{ref}})^2]^{1/2}, \tag{41}$$

$$C^*_{i,\mathrm{test}} = [(a^*_{i,\mathrm{test}})^2 + (b^*_{i,\mathrm{test}})^2]^{1/2}. \tag{42}$$

The differences of the coordinates $(\Delta L^*, \Delta a^*, \Delta b^*)$ between illumination by the reference illuminant and test source for each sample are calculated as follows:

$$\Delta L^*_i = L^*_{i,\mathrm{test}} - L^*_{i,\mathrm{ref}}, \tag{43}$$

$$\Delta a^*_i = a^*_{i,\mathrm{test}} - a^*_{i,\mathrm{ref}}, \tag{44}$$

$$\Delta b^*_i = b^*_{i,\mathrm{test}} - b^*_{i,\mathrm{ref}}. \tag{45}$$

In a similar manner, the difference in chroma between the two illumination conditions, reference and test, is calculated as follows:

$$\Delta C^*_{\mathrm{ab},i} = C^*_{\mathrm{ab},i,\mathrm{test}} - C^*_{\mathrm{ab},i,\mathrm{ref}}. \tag{46}$$

The color difference between illumination by the reference illuminant and test source for each sample is given by

$$\Delta E^*_{\mathrm{ab},i} = [(\Delta L^*_i)^2 + (\Delta a^*_i)^2 + (\Delta b^*_i)^2]^{1/2}. \tag{47}$$

3.5 *Application of the Saturation Factor*

Rather than simply calculating the color difference of each reflective sample as above, a saturation factor is introduced in the calculations of the CQS. The saturation factor serves to negate any contribution to the color difference that arises from an increase in object chroma from test source illumination (relative to the reference illuminant). As discussed earlier, evidence suggests that increases in object chroma, as long as they are not excessive, are not detrimental to color quality and may even be beneficial. Taking the middle ground, with the implementation of the saturation factor, a test source that increases object chroma is not penalized, but is also not rewarded. The color difference for each sample (i) illuminated by the test source and reference illuminant are calculated, with the integration of the saturation factor ($\Delta E^*_{\mathrm{ab},i,\mathrm{sat}}$) is calculated by

$$\Delta E^*_{\mathrm{ab},i,\mathrm{sat}} = \Delta E^*_{\mathrm{ab},i} \quad \text{if} \quad \Delta C^*_{\mathrm{ab},i} \leq 0, \tag{48}$$

$$\Delta E^*_{\mathrm{ab},i,\mathrm{sat}} = [(\Delta E^*_{\mathrm{ab},i})^2 - (\Delta C^*_{\mathrm{ab},i})^2]^{1/2} \quad \text{if} \quad \Delta C^*_{\mathrm{ab},i} > 0. \tag{49}$$

3.6 *Root Mean Square*

All the previous mathematical steps are performed for each of the reflective samples. In the calculation of the General Color Quality Scale (Q_a), the color differences from all 15 samples are considered. If the color differences were merely combined by averaging all 15 color differences, then the Q_a score could be still relatively high even if one or two color samples show very large color differences. This situation is entirely possible with the notable peaks and valleys of RGB LEDs, which can render a couple of object colors poorly, while performing well for all other object colors. To ensure that poor rendering of even a few object colors has a significant impact on the General Color Quality Scale, the color differences are combined by root mean square (rms),

$$\Delta E_{\mathrm{rms}} = \sqrt{\frac{1}{15}\sum_{i=1}^{15} (\Delta E^*_{\mathrm{ab},i,\mathrm{sat}})^2}. \tag{50}$$

3.7 *Scaling Factor*

The "rms average" CQS score is calculated by

$$Q_{\mathrm{a,rms}} = 100 - 3.1 \times \Delta E_{\mathrm{rms}}. \tag{51}$$

The 3.1 in Eq. (51) is the scaling factor, similar to the value 4.6 used in the calculation of CRI [Eq. (1)]. The

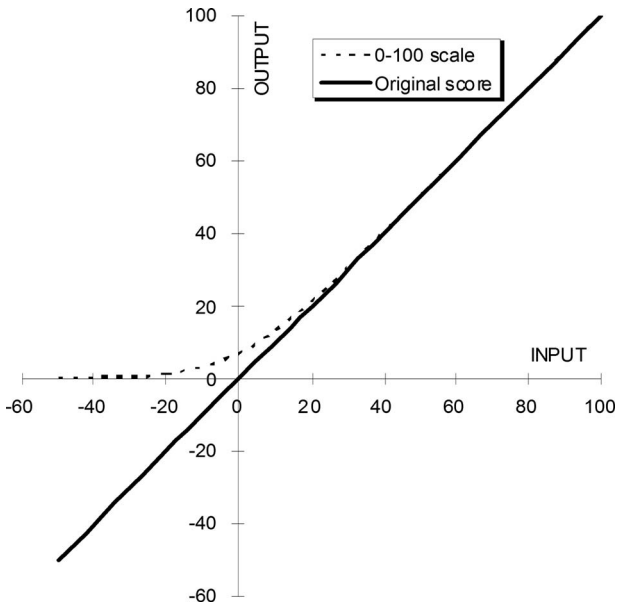

Fig. 5 The 0–100 scale function (dashed) used to convert original scores (solid).

scaling factor for the CRI was selected such that a halophosphate warm white lamp would receive a R_a value of 51.[26] The scaling factor for the CQS was selected so that the average of the General Color Quality Scales (Q_a) for a set of CIE standard fluorescent lamp spectra (F1–F12)[5] is equal to the average output of the CRI (R_a=75.1) for these sources. Though the average scores remain the same for these representative fluorescent lamp spectra, scores for individual lamps are not identical. This selection was intended to maintain a certain degree of consistency between the CRI and CQS in real use and minimize the changes of values from CRI to CQS for traditional light sources.

3.8 *0–100 Scale Conversion*

The CRI can give negative values, which is not desired. Because the basic structure of the calculations are the same for the CRI and CQS, the CQS would also yield negative results for very poor color-rendering sources. To avoid occurrences of such negative numbers, a mathematical function, as follows, is implemented

$$Q_{a,0-100} = 10 \ln\{\exp(Q_{a,rms}/10) + 1\}. \quad (52)$$

The input and output relationship of this formula is shown in Fig. 5. As shown in the figure, only scores lower than ~30 are affected by this conversion and higher values are scarcely affected. Because such low scores only apply to lamps with truly poor color quality, the linearity of the scale at the very bottom is deemed unimportant.

3.9 *CCT Factor*

One final multiplication factor addresses the fact that the reference illuminant (with its CCT matched to that of the test source) always has a perfect score (=100) for any CCT. This variable, called the CCT factor, was devised to penalize lamps with extremely low CCTs, which have smaller gamut areas (and, therefore, render fewer object colors) and exhibit decreased chromatic discrimination performance. This factor is calculated only from the gamut area of the reference source and given by

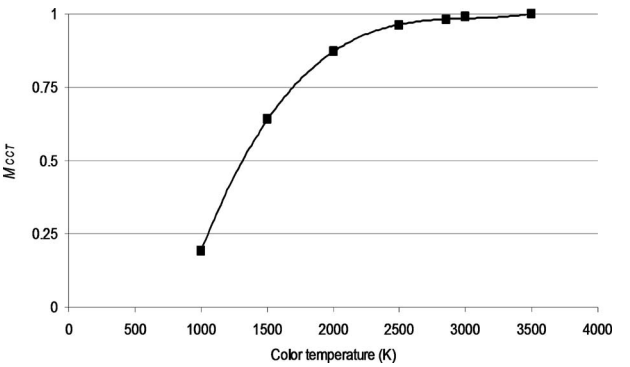

Fig. 6 CCT factor (M_{CCT}) as a function of color temperature for reference illuminants ≤3500 K.

$$M_{CCT} = T^3(9.2672 \times 10^{-11}) - T^2(8.3959 \times 10^{-7}) + T(0.00255) - 1.612 \quad (\text{for } T < 3500 \text{ K}), \quad (53)$$

$$M_{CCT} = 1 \ (\text{for } T \geqslant 3500 \text{ K}), \quad (54)$$

where T is the CCT of the test light source. The derivation of this equation is given in Appendix B, which need not be repeated by the users of the CQS. As shown in Fig. 6, the CCT factor has little impact on white-light sources of practical CCT range (less than two Q_a points are lost for sources $T>2800$ K) but will penalize the light sources having much lower CCTs.

3.10 *General CQS*

Finally, the General CQS (Q_a) is calculated as follows:

$$Q_a = M_{CCT} Q_{a,0-100}. \quad (55)$$

3.11 *Special CQS*

Similar to the CRI, the CQS values for individual test samples are calculated to allow more detailed evaluation of color quality. Using the same scaling factor, the 0–100 conversion formula, and the CCT factor described above, the Special CQS (Q_i) for each reflective sample i is calculated by

$$Q_{i,PRE} = 100 - 3.1 \times \Delta E^*_{ab,i,sat}, \quad (56)$$

$$Q_{i,0-100} = 10(\ln \exp(Q_{i,PRE}/10) + 1), \quad (57)$$

$$Q_i = M_{CCT} Q_{i,0-100}. \quad (58)$$

4 Additional Scales

Though it was emphasized that the CQS must have a one-number output, it is acknowledged that certain applications (e.g., quality control in factories) will require more specific information about the color-rendering properties of light sources. Therefore, for expert users, three additional indices

(described below) are made available from the CQS calculations. These additional scales are also calculated in the CQS spreadsheet available from the authors.

4.1 *Color Fidelity Scale Q_f*

The Color Fidelity Scale (Q_f) is intended to evaluate the fidelity of object color appearances (compared to the reference illuminant of the same CCT and illuminance), similar to the function of CRI R_a. Q_f is calculated using exactly the same procedures as the CQS Q_a, except that it excludes the saturation factor; thus, the equations in Section 3.5 are skipped and the following is used in all cases regardless of the direction of sample chroma shifts:

$$\Delta E^*_{\mathrm{ab},i,\mathrm{sat}} = \Delta E^*_{\mathrm{ab},i}. \tag{59}$$

As was done for Q_a, the scores of Q_f are scaled so that the average score for the 12 reference fluorescent lamp spectra (F1–F12 in Ref. 5) is the same as that for CRI R_a (thus, for CQS Q_a). The scaling factor for Q_f in Eq. (51) is changed to 2.93.

4.2 *Color Preference Scale Q_p*

Although the General CQS Q_a was designed to indicate the overall color quality of a light source, the Color Preference Scale (Q_p) places additional weight on preference of object color appearance. This metric is based on the notion that increases in chroma are generally preferred and should be rewarded. Q_p is calculated using exactly the same procedures as the CQS Q_a, except that it rewards light sources for increasing object chroma; thus, Eq. (51) in Section 3.7 is replaced by

$$Q_{\mathrm{a,rms}} = 100 - 3.78 \times \left[\Delta E_{\mathrm{rms}} - \frac{1}{15}\sum_{i=1}^{15} \Delta C^*_{\mathrm{ab}} \cdot K(i) \right], \tag{60}$$

where

$$K(i) = 1 \quad \text{for } C^*_{\mathrm{ab,test}} \geqslant C^*_{\mathrm{ab,ref}}, \tag{61}$$

$$K(i) = 0 \quad \text{for } C^*_{\mathrm{ab,test}} < C^*_{\mathrm{ab,ref}}. \tag{62}$$

As was done for Q_a, the scores of Q_p are rescaled (scaling factor of 3.78) so that the average score for the 12 reference fluorescent lamp spectra (F1–F12 in Ref. 5) is the same as that for CRI R_a.

4.3 *Gamut Area Scale Q_g*

The Gamut Area Scale (Q_g) is calculated as the relative gamut area formed by the (a^*,b^*) coordinates of the 15 samples illuminated by the test light source in the CIELAB object color space. Q_g is normalized by the gamut area of D65 multiplied by 100; therefore, its scaling is different from Q_a, Q_f, and Q_p and can be $\geqslant$100. See Appendix B for the equations to calculate the gamut area formed by the 15 samples. Note that the chromatic adaptation transform to D65 (used in the derivation of the CCT factor) is not used in Q_g. Q_g is calculated directly from the (a^*,b^*) coordinates calculated in Section 3.4.

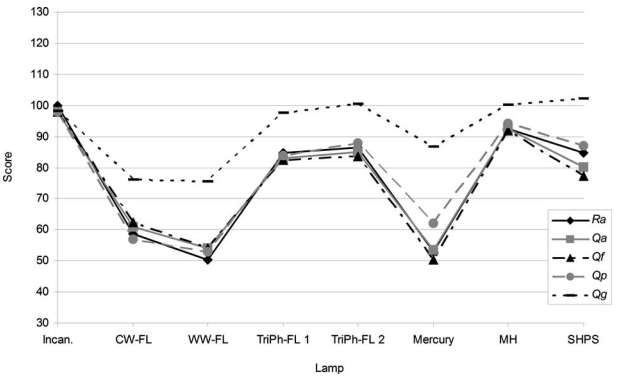

Fig. 7 Comparison of Q_a (gray squares) and R_a (black diamonds) for several traditional lamps including fluorescent and other discharge lamps. Q_f (black triangles), Q_p (gray circles), and Q_g (black dashes) are also shown.

In some cases, RGB white-light spectra can have large gamut areas by increasing object chroma in the red and green regions. Larger gamut areas are always accompanied by corresponding hue shifts. Thus, by looking at the relative gamut area Q_g and knowing the type of light source, one can develop a reasonable estimate of the shape of (a^*,b^*) plot profile for the 15 samples. Note that gamut area does not necessarily correlate well with color preference or color discrimination performance when it is much larger than that of the reference illuminant.

5 Comparison of the CQS and CRI

Although there are several improvements in the CQS over the CRI, one of the most significant changes is the inclusion of the saturation factor, which is effective when light sources enhance object chroma. Because traditional light sources (incandescent and discharge lamps) mostly do not enhance chroma (except the neodymium lamp) and because Q_a is scaled so that the scores for fluorescent lamps will be similar to R_a, the scores of Q_a for traditional lamps are generally very close to R_a. Figure 7 shows the comparison of Q_a and R_a (as well as Q_f, Q_p, and Q_g) for several traditional lamps, including fluorescent and other discharge lamps. The differences are within three points for fluorescent lamps and five points for all these lamps. On the other hand, the CQS shows much larger differences for neodymium lamps and some RGB LED model spectra, as shown in Fig. 8, which shows differences up to 20 points. In addition to RGB LED spectra that enhance object chroma, Fig. 8 shows some RGB LED spectra that have relatively poor color rendering for saturated colors and are scored lower by the CQS than the CRI. The data for the light sources in Fig. 7 and 8 are shown in Table 1. This demonstrates that though the CQS does not deviate substantially from the R_a scores for traditional lamps (this is a requirement for acceptance from the lighting industry), it appropriately treats the chroma-enhancing RGB white LED sources and problematic LED sources.

6 Conclusions

Throughout the development of the calculations of the CQS, computational testing of the performance of the met-

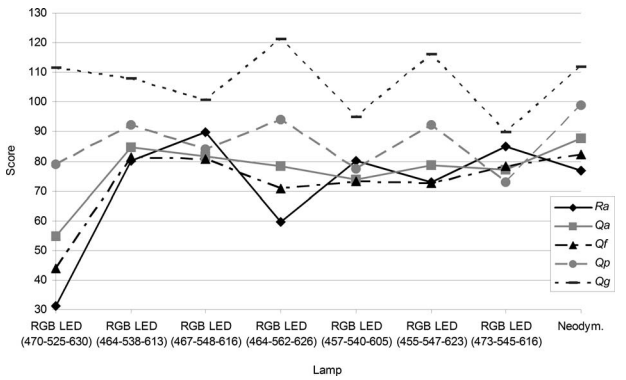

Fig. 8 Comparison of Q_a (gray squares) and R_a (black diamonds) for several RGB LED model spectra. Q_f (black triangles), Q_p (gray circles), and Q_g (black dashes) are also shown.

ric provided feedback as to whether elements of the calculations were effective at enabling the CQS to meet its goals (discussed in Section 2).

Let us revisit the RGB LED shown in Fig. 2. As discussed earlier, this source would receive an R_a score of 80, though it performs very poorly for saturated red and purple reflective samples. Due in large part to the saturated set of reflective samples and the rms combination of color differences, the Q_a score for this RGB LED would be 73. This lower score is far more appropriate and communicates to users how this particular RGB LED performs at color rendering compared to other lamps.

The RGB LED shown in Fig. 3 would receive a R_a of only 67 despite its reasonable overall color quality. In this case, the CQS would give this light source a Q_a of 79. Though the 12 point score increase is notable, the CQS still penalizes this chroma-enhancing source for its hue shifts. Simulations have shown that all light spectra that enhance object chroma also induce comparable hue shifts. Therefore, a chroma-enhancing source will never receive a Q_a of 100. The purpose of the saturation factor is not to favor chroma-enhancing sources, but merely to limit the extent to which they are penalized. This RGB LED illustrates that this objective is met by the CQS. A similar example is the neodymium lamp, which is given CQS Q_a=88, an 11-point increase from CRI R_a=77.

The new metric will serve not only RGB LEDs but also phosphor-type white LEDs, which are presently more dominant in lighting products. Currently available white LEDs use broadband phosphors, but it is foreseen that phosphor LEDs will employ narrowband phosphors in the future, which would have the same problems with CRI as the RGB LEDs. Fluorescent lamps followed such a path of development. They were initially developed using broad-

Table 1 Detailed information on light sources used for Figs. 7 and 8.

Lamp	Details	CCT	R_a	Q_a	Q_f	Q_p	Q_g
Incan.		2812	100	98	98	98	98
CW-FL	F34/CW/RS/EW	4196	59	61	62	57	76
WW-FL	F34T12WW/RS/EW	3011	50	54	54	53	76
TriPh-FL 1	F32T8/TL841	3969	85	83	83	84	98
TriPh-FL 2	F32T8/TL850	5072	86	85	84	88	101
Mercury	H38JA-100/DX	3725	53	53	50	62	87
MH	MHC100/U/MP/4K	4167	92	92	92	94	100
SHPS	SDW-T 100W/LV	2508	85	80	77	87	102
RGB LED (470-525-630)	Simulation	3018	31	55	44	79	111
RGB LED (464-538-613)	Simulation	3300	80	85	81	92	108
RGB LED (467-548-616)	Simulation	3300	90	82	81	84	101
RGB LED (464-562-626)	Simulation	3300	59	78	71	94	121
RGB LED (457-540-605)	Simulation	3300	80	74	73	77	95
RGB LED (455-547-623)	Simulation	3300	73	79	73	92	116
RGB LED (473-545-616)	Simulation	3304	85	77	78	73	90
Neodym.	Incandescent type	2757	77	88	82	99	112

band phosphors but currently employ primarily narrowband phosphors for improved energy efficiency and color rendering.

Though the approach for developing the CQS relied heavily on computational analyses, visual experiments to test, validate, and improve the performance of the CQS are underway. This is a necessary step to ultimately assess and verify the performance of this metric.

Appendix A. Spectral Reflectance Factors for 15 CQS Samples

Wavelength (nm)	7.5P 4/10	10PB 4/10	5PB 4/2	7.5B 5/10	10BG 6/8	2.5BG 6/10	2.5G 6/12	7.5GY 7/10
380	0.1086	0.1053	0.0858	0.079	0.1167	0.0872	0.0726	0.0652
385	0.138	0.1323	0.099	0.0984	0.1352	0.1001	0.076	0.0657
390	0.1729	0.1662	0.1204	0.1242	0.1674	0.1159	0.0789	0.0667
395	0.2167	0.2113	0.1458	0.1595	0.2024	0.1339	0.0844	0.0691
400	0.2539	0.2516	0.1696	0.1937	0.2298	0.1431	0.0864	0.0694
405	0.2785	0.2806	0.1922	0.2215	0.2521	0.1516	0.0848	0.0709
410	0.2853	0.2971	0.2101	0.2419	0.2635	0.157	0.0861	0.0707
415	0.2883	0.3042	0.2179	0.2488	0.2702	0.1608	0.0859	0.0691
420	0.286	0.3125	0.2233	0.2603	0.2758	0.1649	0.0868	0.0717
425	0.2761	0.3183	0.2371	0.2776	0.2834	0.1678	0.0869	0.0692
430	0.2674	0.3196	0.2499	0.2868	0.2934	0.1785	0.0882	0.071
435	0.2565	0.3261	0.2674	0.3107	0.3042	0.1829	0.0903	0.0717
440	0.2422	0.3253	0.2949	0.3309	0.3201	0.1896	0.0924	0.0722
445	0.2281	0.3193	0.3232	0.3515	0.3329	0.2032	0.0951	0.0737
450	0.214	0.3071	0.3435	0.3676	0.3511	0.212	0.0969	0.0731
455	0.2004	0.2961	0.3538	0.3819	0.3724	0.2294	0.1003	0.0777
460	0.1854	0.2873	0.3602	0.4026	0.4027	0.2539	0.1083	0.0823
465	0.1733	0.2729	0.3571	0.4189	0.4367	0.2869	0.1203	0.0917
470	0.1602	0.2595	0.3511	0.4317	0.4625	0.317	0.1383	0.1062
475	0.1499	0.2395	0.3365	0.4363	0.489	0.357	0.1634	0.1285
480	0.1414	0.2194	0.3176	0.4356	0.5085	0.3994	0.1988	0.1598
485	0.1288	0.1949	0.2956	0.4297	0.5181	0.4346	0.2376	0.1993
490	0.1204	0.1732	0.2747	0.4199	0.5243	0.4615	0.2795	0.2445
495	0.1104	0.156	0.2506	0.4058	0.5179	0.4747	0.3275	0.2974
500	0.1061	0.1436	0.2279	0.3882	0.5084	0.4754	0.3671	0.3462
505	0.1018	0.1305	0.2055	0.366	0.4904	0.4691	0.403	0.3894
510	0.0968	0.1174	0.1847	0.3433	0.4717	0.4556	0.4201	0.418
515	0.0941	0.1075	0.1592	0.3148	0.4467	0.4371	0.4257	0.4433
520	0.0881	0.0991	0.1438	0.289	0.4207	0.4154	0.4218	0.4548
525	0.0842	0.0925	0.1244	0.2583	0.3931	0.3937	0.409	0.4605
530	0.0808	0.0916	0.1105	0.234	0.3653	0.3737	0.3977	0.4647
535	0.0779	0.0896	0.0959	0.2076	0.3363	0.3459	0.3769	0.4626
540	0.0782	0.0897	0.0871	0.1839	0.3083	0.3203	0.3559	0.4604
545	0.0773	0.0893	0.079	0.1613	0.2808	0.2941	0.3312	0.4522
550	0.0793	0.0891	0.0703	0.1434	0.2538	0.2715	0.3072	0.4444
555	0.079	0.0868	0.0652	0.1243	0.226	0.2442	0.2803	0.4321
560	0.0793	0.082	0.0555	0.1044	0.2024	0.2205	0.2532	0.4149
565	0.0806	0.0829	0.0579	0.0978	0.1865	0.1979	0.2313	0.4039
570	0.0805	0.0854	0.0562	0.091	0.1697	0.18	0.2109	0.3879
575	0.0793	0.0871	0.0548	0.0832	0.1592	0.161	0.1897	0.3694
580	0.0803	0.0922	0.0517	0.0771	0.1482	0.1463	0.1723	0.3526
585	0.0815	0.0978	0.0544	0.0747	0.1393	0.1284	0.1528	0.3288
590	0.0842	0.1037	0.0519	0.0726	0.1316	0.1172	0.1355	0.308

Wavelength (nm)	7.5P 4/10	10PB 4/10	5PB 4/2	7.5B 5/10	10BG 6/8	2.5BG 6/10	2.5G 6/12	7.5GY 7/10
595	0.0912	0.1079	0.052	0.0682	0.1217	0.1045	0.1196	0.2829
600	0.1035	0.1092	0.0541	0.0671	0.1182	0.0964	0.105	0.2591
605	0.1212	0.1088	0.0537	0.066	0.1112	0.0903	0.0949	0.2388
610	0.1455	0.1078	0.0545	0.0661	0.1071	0.0873	0.0868	0.2228
615	0.1785	0.1026	0.056	0.066	0.1059	0.0846	0.0797	0.2109
620	0.2107	0.0991	0.056	0.0653	0.1044	0.0829	0.0783	0.2033
625	0.246	0.0995	0.0561	0.0644	0.1021	0.0814	0.0732	0.1963
630	0.2791	0.1043	0.0578	0.0653	0.0991	0.0805	0.0737	0.1936
635	0.3074	0.1101	0.0586	0.0669	0.1	0.0803	0.0709	0.1887
640	0.333	0.1187	0.0573	0.066	0.098	0.0801	0.0703	0.1847
645	0.3542	0.1311	0.0602	0.0677	0.0963	0.0776	0.0696	0.1804
650	0.3745	0.143	0.0604	0.0668	0.0997	0.0797	0.0673	0.1766
655	0.392	0.1583	0.0606	0.0693	0.0994	0.0801	0.0677	0.1734
660	0.4052	0.1704	0.0606	0.0689	0.1022	0.081	0.0682	0.1721
665	0.4186	0.1846	0.0595	0.0676	0.1005	0.0819	0.0665	0.172
670	0.4281	0.1906	0.0609	0.0694	0.1044	0.0856	0.0691	0.1724
675	0.4395	0.1983	0.0605	0.0687	0.1073	0.0913	0.0695	0.1757
680	0.444	0.1981	0.0602	0.0698	0.1069	0.093	0.0723	0.1781
685	0.4497	0.1963	0.058	0.0679	0.1103	0.0958	0.0727	0.1829
690	0.4555	0.2003	0.0587	0.0694	0.1104	0.1016	0.0757	0.1897
695	0.4612	0.2034	0.0573	0.0675	0.1084	0.1044	0.0767	0.1949
700	0.4663	0.2061	0.0606	0.0676	0.1092	0.1047	0.081	0.2018
705	0.4707	0.212	0.0613	0.0662	0.1074	0.1062	0.0818	0.2051
710	0.4783	0.2207	0.0618	0.0681	0.1059	0.1052	0.0837	0.2071
715	0.4778	0.2257	0.0652	0.0706	0.1082	0.1029	0.0822	0.2066
720	0.4844	0.2335	0.0647	0.0728	0.1106	0.1025	0.0838	0.2032
725	0.4877	0.2441	0.0684	0.0766	0.1129	0.1008	0.0847	0.1998
730	0.4928	0.255	0.0718	0.0814	0.1186	0.1036	0.0837	0.2024
735	0.496	0.2684	0.0731	0.0901	0.1243	0.1059	0.0864	0.2032
740	0.4976	0.2862	0.0791	0.1042	0.1359	0.1123	0.0882	0.2074
745	0.4993	0.3086	0.0828	0.1228	0.1466	0.1175	0.0923	0.216
750	0.5015	0.3262	0.0896	0.1482	0.1617	0.1217	0.0967	0.2194
755	0.5044	0.3483	0.098	0.1793	0.1739	0.1304	0.0996	0.2293
760	0.5042	0.3665	0.1063	0.2129	0.1814	0.133	0.1027	0.2378
765	0.5073	0.3814	0.1137	0.2445	0.1907	0.1373	0.108	0.2448
770	0.5112	0.3974	0.1238	0.2674	0.1976	0.1376	0.1115	0.2489
775	0.5147	0.4091	0.1381	0.2838	0.1958	0.1384	0.1118	0.2558
780	0.5128	0.4206	0.1505	0.2979	0.1972	0.139	0.1152	0.2635
785	0.5108	0.423	0.1685	0.3067	0.2018	0.1378	0.1201	0.2775
790	0.5171	0.4397	0.1862	0.3226	0.2093	0.1501	0.1253	0.2957
795	0.5135	0.4456	0.2078	0.3396	0.2161	0.1526	0.1313	0.3093
800	0.5191	0.4537	0.2338	0.3512	0.2269	0.1646	0.1393	0.3239
805	0.5191	0.4537	0.2338	0.3512	0.2269	0.1646	0.1393	0.3239
810	0.5191	0.4537	0.2338	0.3512	0.2269	0.1646	0.1393	0.3239
815	0.5191	0.4537	0.2338	0.3512	0.2269	0.1646	0.1393	0.3239
820	0.5191	0.4537	0.2338	0.3512	0.2269	0.1646	0.1393	0.3239
825	0.5191	0.4537	0.2338	0.3512	0.2269	0.1646	0.1393	0.3239
830	0.5191	0.4537	0.2338	0.3512	0.2269	0.1646	0.1393	0.3239

Wavelength (nm)	2.5GY 8/10	5Y 8.5/12	10YR 7/12	5YR 7/12	10R 6/12	5R 4/14	7.5RP 4/12
380	0.0643	0.054	0.0482	0.0691	0.0829	0.053	0.0908
385	0.0661	0.0489	0.0456	0.0692	0.0829	0.0507	0.1021
390	0.0702	0.0548	0.0478	0.0727	0.0866	0.0505	0.113
395	0.0672	0.055	0.0455	0.0756	0.0888	0.0502	0.128
400	0.0715	0.0529	0.0484	0.077	0.0884	0.0498	0.1359
405	0.0705	0.0521	0.0494	0.0806	0.0853	0.0489	0.1378
410	0.0727	0.0541	0.0456	0.0771	0.0868	0.0503	0.1363
415	0.0731	0.0548	0.047	0.0742	0.0859	0.0492	0.1363
420	0.0745	0.0541	0.0473	0.0766	0.0828	0.0511	0.1354
425	0.077	0.0531	0.0486	0.0733	0.0819	0.0509	0.1322
430	0.0756	0.0599	0.0501	0.0758	0.0822	0.0496	0.1294
435	0.0773	0.0569	0.048	0.0768	0.0818	0.0494	0.1241
440	0.0786	0.0603	0.049	0.0775	0.0822	0.048	0.1209
445	0.0818	0.0643	0.0468	0.0754	0.0819	0.0487	0.1137
450	0.0861	0.0702	0.0471	0.0763	0.0807	0.0468	0.1117
455	0.0907	0.0715	0.0486	0.0763	0.0787	0.0443	0.1045
460	0.0981	0.0798	0.0517	0.0752	0.0832	0.044	0.1006
465	0.1067	0.086	0.0519	0.0782	0.0828	0.0427	0.097
470	0.1152	0.0959	0.0479	0.0808	0.081	0.0421	0.0908
475	0.1294	0.1088	0.0494	0.0778	0.0819	0.0414	0.0858
480	0.141	0.1218	0.0524	0.0788	0.0836	0.0408	0.0807
485	0.1531	0.1398	0.0527	0.0805	0.0802	0.04	0.0752
490	0.1694	0.1626	0.0537	0.0809	0.0809	0.0392	0.0716
495	0.1919	0.1878	0.0577	0.0838	0.0838	0.0406	0.0688
500	0.2178	0.2302	0.0647	0.0922	0.0842	0.0388	0.0678
505	0.256	0.2829	0.0737	0.1051	0.0865	0.0396	0.0639
510	0.311	0.3455	0.0983	0.123	0.091	0.0397	0.0615
515	0.3789	0.4171	0.1396	0.1521	0.092	0.0391	0.0586
520	0.4515	0.4871	0.1809	0.1728	0.0917	0.0405	0.0571
525	0.5285	0.5529	0.228	0.1842	0.0917	0.0394	0.0527
530	0.5845	0.5955	0.2645	0.1897	0.0952	0.0401	0.0513
535	0.6261	0.6299	0.2963	0.1946	0.0983	0.0396	0.0537
540	0.6458	0.6552	0.3202	0.2037	0.1036	0.0396	0.0512
545	0.6547	0.6661	0.3545	0.2248	0.115	0.0395	0.053
550	0.6545	0.6752	0.395	0.2675	0.1331	0.0399	0.0517
555	0.6473	0.6832	0.4353	0.3286	0.1646	0.042	0.0511
560	0.6351	0.6851	0.4577	0.3895	0.207	0.041	0.0507
565	0.6252	0.6964	0.4904	0.4654	0.2754	0.0464	0.0549
570	0.6064	0.6966	0.5075	0.5188	0.3279	0.05	0.0559
575	0.5924	0.7063	0.5193	0.5592	0.3819	0.0545	0.0627
580	0.5756	0.7104	0.5273	0.5909	0.425	0.062	0.0678
585	0.5549	0.7115	0.5359	0.6189	0.469	0.0742	0.081
590	0.5303	0.7145	0.5431	0.6343	0.5067	0.0937	0.1004
595	0.5002	0.7195	0.5449	0.6485	0.5443	0.1279	0.1268
600	0.4793	0.7183	0.5493	0.6607	0.5721	0.1762	0.1595
605	0.4517	0.7208	0.5526	0.6648	0.5871	0.2449	0.2012
610	0.434	0.7228	0.5561	0.6654	0.6073	0.3211	0.2452
615	0.4169	0.7274	0.5552	0.6721	0.6141	0.405	0.2953
620	0.406	0.7251	0.5573	0.6744	0.617	0.4745	0.3439

Wavelength (nm)	2.5GY 8/10	5Y 8.5/12	10YR 7/12	5YR 7/12	10R 6/12	5R 4/14	7.5RP 4/12
625	0.3989	0.7274	0.562	0.6723	0.6216	0.5335	0.3928
630	0.3945	0.7341	0.5607	0.6811	0.6272	0.5776	0.4336
635	0.3887	0.7358	0.5599	0.6792	0.6287	0.6094	0.4723
640	0.3805	0.7362	0.5632	0.6774	0.6276	0.632	0.4996
645	0.3741	0.7354	0.5644	0.6796	0.6351	0.6495	0.5279
650	0.37	0.7442	0.568	0.6856	0.6362	0.662	0.5428
655	0.363	0.7438	0.566	0.6853	0.6348	0.6743	0.5601
660	0.364	0.744	0.5709	0.6864	0.6418	0.6833	0.5736
665	0.359	0.7436	0.5692	0.6879	0.6438	0.6895	0.5837
670	0.3648	0.7442	0.5657	0.6874	0.6378	0.6924	0.589
675	0.3696	0.7489	0.5716	0.6871	0.641	0.703	0.5959
680	0.3734	0.7435	0.5729	0.6863	0.646	0.7075	0.5983
685	0.3818	0.746	0.5739	0.689	0.6451	0.7112	0.6015
690	0.3884	0.7518	0.5714	0.6863	0.6432	0.7187	0.6054
695	0.3947	0.755	0.5741	0.6893	0.6509	0.7214	0.6135
700	0.4011	0.7496	0.5774	0.695	0.6517	0.7284	0.62
705	0.404	0.7548	0.5791	0.6941	0.6514	0.7327	0.6287
710	0.4072	0.7609	0.5801	0.6958	0.6567	0.7351	0.6405
715	0.4065	0.758	0.5804	0.695	0.6597	0.7374	0.6443
720	0.4006	0.7574	0.584	0.7008	0.6576	0.741	0.6489
725	0.3983	0.7632	0.5814	0.702	0.6576	0.7417	0.6621
730	0.3981	0.7701	0.5874	0.7059	0.6656	0.7491	0.6662
735	0.399	0.7667	0.5885	0.7085	0.6641	0.7516	0.6726
740	0.4096	0.7735	0.5911	0.7047	0.6667	0.7532	0.6774
745	0.4187	0.772	0.5878	0.7021	0.6688	0.7567	0.6834
750	0.4264	0.7739	0.5896	0.7071	0.6713	0.76	0.6808
755	0.437	0.774	0.5947	0.7088	0.6657	0.7592	0.6838
760	0.4424	0.7699	0.5945	0.7055	0.6712	0.7605	0.6874
765	0.4512	0.7788	0.5935	0.7073	0.6745	0.7629	0.6955
770	0.4579	0.7801	0.5979	0.7114	0.678	0.7646	0.7012
775	0.4596	0.7728	0.5941	0.7028	0.6744	0.7622	0.6996
780	0.4756	0.7793	0.5962	0.7105	0.6786	0.768	0.7023
785	0.488	0.7797	0.5919	0.7078	0.6823	0.7672	0.7022
790	0.5066	0.7754	0.5996	0.7112	0.6806	0.7645	0.7144
795	0.5214	0.781	0.5953	0.7123	0.6718	0.7669	0.7062
800	0.545	0.7789	0.5953	0.7158	0.6813	0.7683	0.7075
805	0.545	0.7789	0.5953	0.7158	0.6813	0.7683	0.7075
810	0.545	0.7789	0.5953	0.7158	0.6813	0.7683	0.7075
815	0.545	0.7789	0.5953	0.7158	0.6813	0.7683	0.7075
820	0.545	0.7789	0.5953	0.7158	0.6813	0.7683	0.7075
825	0.545	0.7789	0.5953	0.7158	0.6813	0.7683	0.7075
830	0.545	0.7789	0.5953	0.7158	0.6813	0.7683	0.7075

Appendix B. Calculation of CCT Factor

The CCT factor is based on the relative gamut area of the reference illuminant as a function of its CCT. First, the X,Y,Z tristimulus values of the 15 reflective samples under the reference illuminant are converted to their color appearance under D65 using CMCCAT2000 chromatic adaptation transform[23] (see Section 3.3). This is done because CIELAB was designed for best performance with D65, and the gamut areas of a wide range of CCTs can be more accurately evaluated using this conversion.

Then, the gamut area of the 15 CQS samples in CIELAB (a^*,b^*) space (see Section 3.4) is calculated for the reference illuminant at the given CCT. The gamut area is divided into 15 triangles (S), each of which is formed by two

Table 2 Gamut areas and CCT factors (M_{CCT}) for a number of CCTs.

CCT (K)	Gamut Area	M_{CCT}
1000	1579	0.19
1500	5293	0.65
2000	7148	0.87
2500	7858	0.96
2856	8085	0.99
3000	8144	0.99
3500	8267	1.00
4000	8322	1.00
5000	8354	1.00
6000	8220	1.00
6500	8210	1.00
7000	8202	1.00
8000	8191	1.00
9000	8185	1.00
10,000	8181	1.00
15,000	8180	1.00
20,000	8183	1.00

neighboring points of the (a^*,b^*) plot and the origin. The calculation of the area of each triangle $(i=1-15)$ is done by

$$A_i = [(a^*_{i,\mathrm{ref}})^2 + (b^*_{i,\mathrm{ref}})^2]^{1/2}, \tag{63}$$

$$B_i = [(a^*_{i+1,\mathrm{ref}})^2 + (b^*_{i+1,\mathrm{ref}})^2]^{1/2}, \tag{64}$$

$$C_i = [(a^*_{i+1,\mathrm{ref}} - a^*_{i,\mathrm{ref}})^2 + (b^*_{i+1,\mathrm{ref}} - b^*_{i,\mathrm{ref}})^2]^{1/2}. \tag{65}$$

For $i=15$, $i+1$ is replaced by 1,

$$t_i = \frac{A_i + B_i + C_i}{2}, \tag{66}$$

$$S_i = [t_i(t_i - A_i)(t_i - B_i)(t_i - C_i)]^{1/2}. \tag{67}$$

The areas of all the triangles are summed to calculate the total gamut area (G)

$$G = \sum_{i=1}^{15} S_i. \tag{68}$$

To determine the CCT factor, the gamut area of the reference illuminant is normalized to that of D65 (=8210 CIELAB units). If the gamut area of the reference illuminant is greater than that of D65, the multiplication factor is simply set to 1,

$$M_{CCT} = 1 \quad \text{if } G \geqslant 8210, \tag{69}$$

$$M_{CCT} = \frac{G}{8210} \quad \text{if } G < 8210. \tag{70}$$

The results of the CCT factor calculations are shown in Table 2 for a number of CCT values. It only needs to be calculated for CCTs of <3500 K. A curve fit to the points for illuminants of <4000 K in Table 2, as shown in Fig. 6, was obtained with a third-order polynomial with $R^2 = 0.9999$

$$M_{CCT} = T^3(9.2672 \times 10^{-11}) - T^2(8.3959 \times 10^{-7}) + T(0.00255) - 1.612, \tag{71}$$

where T is the CCT of the reference illuminant. This function fits the data well, and this polynomial can be used to determine the CCT factor for sources of <3500 K, eliminating the need for Eqs. (63)–(70).

References

1. CIE 17.4: 1987, "International lighting vocabulary," Item No. 845-02-59 (1987).
2. CIE 13.3: 1995, "Method of measuring and specifying colour rendering properties of light sources" (1995).
3. Y. Ohno, "Spectral design considerations for color rendering of white LED light sources," *Opt. Eng.* **44**(11), 111302 (2005).
4. CIE 177: 2007, "Colour rendering of white LED light sources" (2007).
5. CIE 15: 2004, "Colorimetry" ⟨http://www.cie.co.at/main/freepubs.html⟩ (2004).
6. CIE 160: 2004, "A review of chromatic adaptation transforms" (2004).
7. K. Hashimoto, T. Yano, M. Shimizu, and Y. Nayatani, "New method for specifying color-rendering properties of light sources based on feeling of contrast," *Color Res. Appl.* **32**, 361–371 (2007).
8. L. Booker, "Luminance-brightness comparisons of separated circular stimuli," *J. Opt. Soc. Am.* **71**, 139–144 (1981).
9. D. B. Judd, "A flattery index for artificial illuminants," *Illum. Eng. (N.Y.)* **62**, 593–598 (1967).
10. C. L. Sanders, "Color preferences for natural objects," *Illum. Eng. (N.Y.)* **54**, 452–456 (1959).
11. S. M. Newhall, R. W. Burnham, and J. R. Clark, "Comparison of successive with simultaneous color matching," *J. Opt. Soc. Am.* **47**, 43–56 (1957).
12. W. A. Thorton, "A validation of the color preference index," *J. Illum. Eng.* **4**, 48–52 (1974).
13. C. J. Bartleson, "Color in memory in relation to photographic reproduction," *Photograph. Sci. Eng.* **5**, 327–331 (1961).
14. J. Schanda, "A combined colour preference—colour rendering index," *Light. Res. Technol.* **17**, 31–34 (1985).
15. W. von Bezold, "Über das Gesetz der Farbenmischung und die physiologischen Grundfarben," *Annal. Physiol. Chemie* **226**, 221–247 (1873).
16. R. W. G. Hunt, "Light and dark adaptation and the perception of color," *J. Opt. Soc. Am.* **42**, 190–199 (1952).
17. S. M. Aston and H. E. Bellchamber, "Illumination, color rendering and visual clarity," *Light. Res. Technol.* **1**, 259–261 (1969).
18. P. R. Boyce, "Investigations of the subjective balance between illuminance and lamp colour properties," *Light. Res. Technol.* **9**, 11–24 (1977).
19. W. A. Thornton, "Color-discrimination index," *J. Opt. Soc. Am.* **62**, 191–194 (1972).
20. H. Xu, "Colour rendering capacity and luminous efficiency of a spectrum," *Light. Res. Technol.* **25**, 131–32 (1993).
21. S. A. Fotios and G. J. Levermore, "Perception of electric light sources of different colour properties," *Light. Res. Technol.* **29**, 161–171 (1997).
22. J. A. Worthey, "Color rendering: asking the question," *Color Res. Appl.* **28**, 403–412 (2003).
23. M. S. Rea and J. P. Freyssinier-Nova, "A tale of two metrics," *Color*

Res. Appl. **33**, 192–200 (2008).
24. CIE 167: 2005, "Recommended practice for tabulating spectral data for use in color computations" (2005).
25. C. J. Li, M. R. Luo, B. Rigg, and R. W. G. Hunt, "CMC 2000 chromatic adaptation transform: CMCCAT2000," *Color Res. Appl.* **27**, 49–58 (2002).
26. J. Schanda and N. Sándor, "Colour rendering, past-present-future," in *Proc. of Int. Lighting and Colour Conf.*, pp. 76–85, SANCI, Cape Town, South Africa (2003).

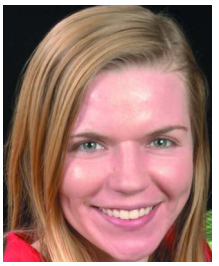

Wendy Davis is a vision scientist in the Optical Technology Division at the National Institute of Standards and Technology (NIST). She joined NIST soon after completing her PhD in vision science at the University of California, Berkeley, in 2004. Dr. Davis and her colleagues in colorimetry and photometry are currently establishing a permanent Vision Science Program at NIST. Her current main research focus is the development of a color quality metric, suitable for both solid state lighting, and traditional lamps.

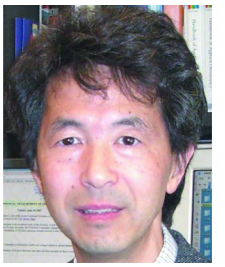

Yoshi Ohno is the group leader of Optical Sensor Group, Optical Technology Division of NIST. His group is responsible for maintaining national standards of the candela, lumen, and color scales. He serves as the director of CIE Division 2 and active in many national and international committees in ANSI, IESNA, CIE, CIPM, and IEC on optical metrology and standardization of solid state lighting.